

Linear and Non-linear Analyses of Double Diffusive Chandrasekhar Convection with Heat and Concentration Source in Micropolar Fluid with Saturated Porous Media under Gravity Modulation

S Maria Anncy, T V Joseph and S Pranesh

Abstract—In this paper, linear and non-linear analysis of Double-Diffusive convection in the presence of magnetic field and gravity modulation with heat and concentration source in a micropolar fluid is studied by assuming the strength of heat and concentration source same. The expression for Rayleigh number and correction Rayleigh number are obtained using regular perturbation method. The effects of parameters on heat and mass transport is investigated using non-linear analysis by deriving eighth order Lorenz equation. It is found that coupling parameter and Chandrasekhar number stabilizes the system. Whereas internal Rayleigh number and Darcy number destabilizes the system.

Index Terms—double diffusive Chandrasekhar convection, temperature and concentration based internal heat source, micropolar fluid, porous media, gravity modulation.

I. INTRODUCTION

MANY practical important fluid mechanics problems involve the flow through porous medium. The storage and movement of fluid in porous medium are controlled by porosity and permeability of the porous medium. The flow through porous medium has been extensively studied because of its applications in science and engineering (see Nield and Bejan [1]). The important topic discussed in this paper is the convective heat and mass transport in a porous medium in the presence of heat and concentration source and gravity modulation. Many authors like Sheremet et al. [2], Sivaraj and Sheremet [3], Miroshnichenko et al. [4], Izadi et al. [5], investigated the flow in a porous medium under different situations.

The presence of two or more components with different molecular diffusivity in a gravitational field developed a new field of convection known as double diffusive convection. In double diffusive convection two types of modes are possible:

- Diffusivity mode – when larger diffusive component is heavier on top and
- Finger mode – when smaller diffusive component is heavy on top.

Oceanography is the primary cause of research in double diffusive convection. In many physical situations such as earth's ocean, crystal growth, geophysical system, chemistry, metallurgy, etc., double diffusive convection arises. The good review of double diffusive phenomenon can be found in

Turner [6] and Huppert and Turner [7]. The development of double diffusive phenomena in oceanography is summarized in detail by Schmitt [8] and its engineering applications by Chen and Johnson [9].

Nield [10] was the first to study the double diffusive convection in porous medium using linear stability analysis for different thermal and solutal boundaries. Later Taunton et al. [11], Rudraiah et al. [12], Poulikakos [13], Rosenberg and Spera [14], Kuznetsor and Nield [15], [16], Rana and Chand [17], Bhadauria et al. [18], Akbar et al. [19], Hameed and Harfash [20], Harfash [21], Garaud [22], Raghunatha and Shivakumara [23] investigated double diffusive convection in porous medium under different situations.

Double diffusive convection occurs due to the interaction of gravity field with gradients of fluid density. Therefore double diffusive convection may be enhanced or reduced by changing gravity. Microgravity environment in space stations will not remain constant, but it fluctuates with amplitude and frequency, this fluctuating gravity is called g-jitter or gravity modulation, which significantly influences natural convection. Therefore, it is very important to understand the effect of gravity modulations on the double diffusive convection phenomena.

Gresho and Sani [24] were first to study the effect of gravity modulation in a fluid layer. Murray et al. [25] using Floquet theory studied the effect of vertical oscillating on solutal convection. Saunders et al. [26] investigated the effect of gravity modulation on the double diffusive convection. Using linear stability analysis, Siddheshwar et al. [27] studied the effect of heat and mass transport in a double diffusive convection with porous medium under gravity modulation. Bhadauria et al. [28], [29], Maria and Sangeetha [30], Purusothaman et al. [31] investigated the effect of time-periodic body force in a horizontal layer of fluid heated from below.

When fluid contains free suspended particles it undergoes translation and rotation relative to the fluid. One way of taking these type of fluids is by modelling through Eringen micropolar fluid. In these type of fluids stress is non-symmetric, hence they do not satisfy the Navier-Stokes equation and these fluids are non-Newtonian in nature. In order to explain the kinematics of these fluids spin and micro inertia are added to velocity. Micropolar fluid theory have innumerable applications in science and engineering (see Lukaszewicz [32]) which motivated many authors Ahamadi [33], Jean and Bhattacharya [34], Datta and Sastry [35], Siddheshwar and Pranesh [36]–[39], Pranesh and Arun Kumar [40], [41],

Manuscript received May 06, 2019; revised November 12, 2019.

S. Maria Anncy, Research Scholar, Department of Mathematics, CHRIST(Deemed to be University), Bangalore, India, e-mail:(maria.anncy@res.christuniversity.in).

T. V. Joseph and S. Pranesh are with CHRIST(Deemed to be University).

Pranesh and Riya Baby [42], Pranesh and Sameena [43] to consider this fluid for their research.

One of the simplest way to control the onset of convection and heat and mass transport is by applying the external magnetic field, which is known as magneto-convection or Chandrasekhar convection. Siddheshwar and Pranesh [36], [37], [39] studied the effect of magnetic field in a micropolar fluid.

The onset of double diffusive convection in a horizontal layer of fluid can be controlled by maintaining the non-uniform temperature gradient (see Siddheshwar and Pranesh [36]) and non-uniform concentration gradient (Pranesh and Arun [40]). These non-linear temperature and concentration distribution arises when there is a presence of heat and concentration source. Many authors have studied the double diffusive convection in the presence of heat source in a porous medium. Hill [44] and Anjanna and Hill [45] investigated the double diffusive convection in the presence of concentration dependent heat source. Although many studies are available on double diffusive convection in a porous medium with internal heat source, no attention is given to study the onset of double diffusive convection in a porous medium in the presence of both internal heat and concentration source.

Thus, the main objective of this paper is to show how the onset of Double-Diffusive-Chandrasekhar convection and heat and mass transport is affected in the presence of internal heat and concentration source in a micropolar fluid under gravity modulation.

II. MATHEMATICAL FORMULATION

The physical configuration of the problem consists of a material with voids which are interconnected between two horizontal parallel plates separated by a distance 'd'. In this problem the voids are filled with micropolar fluid. The system involves magnetic effect based on temperature and concentration internal heat source and is exposed to gravity modulation. The lower plate is considered to be hotter than upper plate and gravity acts downwards. The solute is added from the lower plate. Cartesian coordinates are taken with origin at the lower plate and z-axis along the vertical direction, (see figure-1).

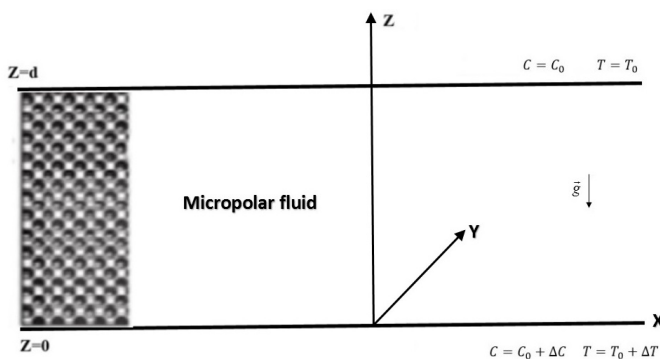


Fig. 1: Physical Configuration

The governing equations of the problem are:

$$\nabla \cdot \vec{q} = 0, \tag{1}$$

$$\rho_0 \left[\frac{1}{\phi} \frac{\partial \vec{q}}{\partial t} + \frac{1}{\phi^2} (\vec{q} \cdot \nabla) \vec{q} \right] = -\nabla P - \rho g_0 [1 + \epsilon \cos(\gamma t)] \hat{k} + \left(\frac{2\zeta}{\phi} + \eta \right) \nabla^2 \vec{q} - \left(\frac{\zeta + \eta}{K} \right) \vec{q} + \zeta \nabla \times \vec{\omega} + \mu_m (\vec{H} \cdot \nabla) \vec{H}, \tag{2}$$

$$\rho_0 I \left[\frac{\partial \vec{\omega}}{\partial t} + \frac{1}{\phi} (\vec{q} \cdot \nabla) \vec{\omega} \right] = (\lambda' + \eta') \nabla (\nabla \cdot \vec{\omega}) + (\eta' \nabla^2 \vec{\omega}) + \frac{\zeta}{\phi} (\nabla \times \vec{q}) - 2\zeta \vec{\omega}, \tag{3}$$

$$\frac{\partial T}{\partial t} + (\vec{q} \cdot \nabla) T = \kappa \nabla^2 T + \frac{\beta}{\rho_0 C_v} (\nabla \times \vec{\omega}) \cdot \nabla T + Q_i (T - T_0), \tag{4}$$

$$\frac{\partial C}{\partial t} + (\vec{q} \cdot \nabla) C = \kappa_s \nabla^2 C + Q_i (C - C_0), \tag{5}$$

$$\nabla \cdot \vec{H} = 0, \tag{6}$$

$$\frac{\partial \vec{H}}{\partial t} + (\vec{q} \cdot \nabla) \vec{H} = (\vec{H} \cdot \nabla) \vec{q} + \gamma_m \nabla^2 \vec{H}, \tag{7}$$

$$\rho = \rho_0 [1 - \alpha_t (T - T_0) + \alpha_s (C - C_0)]. \tag{8}$$

where, \vec{q} is the velocity, $\vec{\omega}$ is the spin, ρ is the density, $P = p + \mu_m \frac{H^2}{2}$ is the hydromagnetic pressure, \vec{H} is the magnetic field, γ_m is the magnetic viscosity co-efficient, T is the temperature, C is the concentration, Q_i is strength of internal heat and concentration source, β is the heat conduction parameter, C_v is the specific heat, ϵ is the amplitude, γ is the frequency, ϕ is the porosity, K is the permeability, g_0 is the acceleration due to gravity. The equations (1)-(8) are solved subjected to stress free isothermal and isoconcentration conditions given by,

$$W = \frac{\partial^2 W}{\partial z^2} = T = C = 0 \text{ at } z = 0 \text{ and } z = d.$$

A. Solution of Motionless State

Considering that the density, pressure, temperature, magnetic field and solutal concentration in motionless state are horizontally linear gradients, the parameters takes the values:

$$\vec{q}_b = 0; \quad \vec{\omega}_b = 0; \quad \vec{H}_b = H_0 \hat{k}; \quad \rho = \rho_b(z); \\ P = P_b(z); \quad T = T_b(z); \quad C = C_b(z).$$

Substituting these in equations (1-8), we get the following solutions of the system in motionless state:

$$-\nabla P_b - \rho_b g_0 = 0, \tag{9}$$

$$\kappa \nabla^2 T_b + Q_i (T_b - T_0) = 0, \tag{10}$$

$$\kappa_s \nabla^2 C_b + Q_i (C_b - C_0) = 0, \tag{11}$$

$$\rho_b = \rho_0 [1 - \alpha_t (T_b - T_0) + \alpha_s (C_b - C_0)]. \tag{12}$$

The motionless state of the system is slightly disturbed and in perturbed state the parameters takes the form:

$$\vec{q} = \vec{q}_b + \vec{q}', \quad \vec{\omega} = \vec{\omega}_b + \vec{\omega}', \quad \vec{H} = \vec{H}_0 \hat{k} + \vec{H}', \quad \rho = \rho_b + \rho', \\ P = P_b + P', \quad T = T_b + T', \quad C = C_b + C'. \tag{13}$$

Substituting equation (13) in equations (1-8), using the motionless state solution and non-dimensionalizing the resultant

equations using the following definitions,

$$q^* = \frac{q'}{\chi/d}, P^* = \frac{P'}{P_0}, T^* = \frac{T'}{\Delta T}, \nabla^* = \nabla d,$$

$$t^* = \frac{t'}{d^2/\kappa}, \omega^* = \frac{\omega'}{\kappa/d^2}, C^* = \frac{C'}{\Delta C}, H^* = \frac{H'}{H_0},$$

$$(x^*, y^*, z^*) = \frac{(x', y', z')}{d}.$$

and introducing the stream functions,

$$u = \frac{\partial \Psi}{\partial z}, w = \frac{-\partial \Psi}{\partial x} \quad \text{and} \quad H_x = \frac{\partial \Phi}{\partial z}, H_z = \frac{-\partial \Phi}{\partial x},$$

we get the following dimensionless equations after neglecting asterisks :

$$\left[\frac{1}{\phi P_r} \frac{\partial}{\partial t} - \Lambda \left(1 + \frac{N_1}{\phi \Lambda} \right) \nabla^2 + Da^{-1} \right] \nabla^2 \Psi =$$

$$\left(-R \frac{\partial T}{\partial x} + R_s \frac{\partial C}{\partial x} \right) \left(1 + \epsilon \cos \omega t \right) - N_1 \nabla^2 \omega_y +$$

$$Q \frac{P_r}{P_m} \nabla^2 \left(\frac{\partial \Phi}{\partial z} \right) - Q \frac{P_r}{P_m} J(\Phi, \nabla^2 \Phi) + \frac{1}{\phi^2 P_r} J(\Psi, \nabla^2 \Psi), \tag{14}$$

$$\left[\frac{N_2}{P_r} \frac{\partial}{\partial t} - N_3 \nabla^2 + 2N_1 \right] \omega_y = \frac{N_1}{\phi} \nabla^2 \Psi + \frac{N_2}{\phi P_r} J(\Psi, \omega_y), \tag{15}$$

$$\left[\frac{\partial}{\partial t} - \nabla^2 - R_i \right] T = -g(z) \left[\frac{\partial \Psi}{\partial x} + N_5 \frac{\partial \omega_y}{\partial x} \right] + N_5 J(\omega_y, T)$$

$$+ J(\Psi, T), \tag{16}$$

$$\left[\frac{\partial}{\partial t} - \tau \nabla^2 - R_i \right] C = -h(z) \frac{\partial \Psi}{\partial x} + J(\Psi, C), \tag{17}$$

$$\left[\frac{\partial}{\partial t} - \frac{P_r}{P_m} \nabla^2 \right] \Phi = \frac{\partial \Psi}{\partial z} + J(\Psi, \Phi). \tag{18}$$

The non-dimensionalized parameters obtained in the above equations are given in Table I.

B. Linear Stability Analysis

In this section, we neglect Jacobians in equations (16)-(20) to consider only the linear terms to obtain the condition for the onset of convection. Eliminating C, T, ω_y , Φ from the resulting equations we get:

$$X_2 \nabla^2 \left\{ X_3 \left[X_1 \nabla^2 \left(X_4 X_5 - Q \frac{P_r}{P_m} \frac{\partial^2}{\partial z^2} \right) + X_5 h(z) R_s \right. \right.$$

$$\left. \left. \left(1 + \epsilon \cos(\gamma t) \right) \right] + X_1 X_5 \frac{N_1^2}{\phi} \nabla^4 \right\} \Psi = R X_1 X_5 g(z)$$

$$\left(1 + \epsilon \cos(\gamma t) \right) \frac{\partial^2}{\partial x^2} \nabla^2 \left[X_3 + \frac{N_1 N_5}{\phi} \nabla^2 \right] \Psi. \tag{19}$$

where,

$$X_1 = \frac{\partial}{\partial t} - \tau \nabla^2 - R_i,$$

TABLE I: Non-dimensionalized parameters

$N_1 = \frac{\zeta}{\zeta + \eta}$	(Coupling parameter)
$N_2 = \frac{d^2}{\eta^2}$	(Inertia parameter)
$N_3 = \frac{d^2}{\mu d^2}$	(Couple stress parameter)
$N_5 = \frac{\beta}{\rho_0 C_v d^2}$	(Micropolar heat conduction parameter)
$Da = \frac{K_1}{d^2}$	(Darcy number)
$P_r = \frac{\zeta + \eta}{\rho_0 \kappa}$	(Prandtl number)
$P_m = \frac{\rho_0 \gamma_m}{\zeta + \eta}$	(Magnetic Prandtl number)
$Q = \frac{\mu_m H_0^2 d^2}{\kappa(\zeta + \eta)}$	(Chandrasekhar number)
$R = \frac{\alpha_t \rho_0 \nabla T g_0 d^3}{\kappa(\zeta + \eta)}$	(Rayleigh number)
$R_s = \frac{\alpha_s \rho_0 \nabla c g_0 d^3}{\kappa(\zeta + \eta)}$	(Solutal Rayleigh number)
$R_i = \frac{Q_i d^2}{\kappa}$	(Internal Rayleigh number)
$\Lambda = \frac{\zeta + \eta}{\phi}$	(Modified viscosity ratio)
$\tau = \frac{\kappa_s}{\kappa}$	(Diffusivity ratio)
$\omega = \frac{\gamma d^2}{\kappa}$	(Internal Rayleigh number)
$h(z) = \frac{\sqrt{R_i} \cos \sqrt{\tau R_i} (1-z)}{\sin \sqrt{\tau R_i}}$	$g(z) = \frac{\sqrt{R_i} \cos \sqrt{R_i} (1-z)}{\sin \sqrt{R_i}}$

$$X_2 = \frac{\partial}{\partial t} - \nabla^2 - R_i,$$

$$X_3 = \frac{N_2}{P_r} \frac{\partial}{\partial t} - N_3 \nabla^2 + 2N_1,$$

$$X_4 = \frac{1}{\phi P_r} \frac{\partial}{\partial t} - \Lambda \left(1 + \frac{N_1}{\Lambda \phi} \right) \nabla^2 + Da^{-1} \quad \text{and}$$

$$X_5 = \frac{\partial}{\partial t} - \frac{P_r}{P_m} \nabla^2.$$

The boundary conditions for solving (21) are obtained as:

$$\Psi = \frac{\partial^2 \Psi}{\partial x^2} = \frac{\partial^4 \Psi}{\partial x^4} = \frac{\partial^6 \Psi}{\partial x^6} = \frac{\partial^8 \Psi}{\partial x^8} = \frac{\partial^{10} \Psi}{\partial x^{10}} = \frac{\partial^{12} \Psi}{\partial x^{12}} = 0$$

at $z = 0$ and $z = 1$. (20)

Following the Venezian [46] approach, we expand eigen value and eigen function as

$$R = R_0 + \epsilon^2 R_2 + \dots \tag{21}$$

$$\Psi = \Psi_0 + \epsilon \Psi_1 + \epsilon^2 \Psi_2 + \dots \tag{22}$$

Substituting (23) and (24) in (21) , equating like powers of ϵ on both sides we get:

$$L_1 \Psi_0 = 0, \tag{23}$$

$$L_1 \Psi_1 = X_5 \cos(\gamma t) \frac{\partial^2}{\partial x^2} \nabla^2 \Psi_0 \left[R_0 g(z) X_1 \left(X_3 + \frac{N_1 N_5}{\phi} \nabla^2 \right) \right. \\ \left. - R_s h(z) X_2 X_3 \right], \tag{24}$$

$$L_1\Psi_2 = X_5 \left\{ \cos(\gamma t) \frac{\partial^2}{\partial x^2} \nabla^2 \Psi_1 \left[R_0 g(z) X_1 \left(X_3 + \frac{N_1 N_5}{\phi} \nabla^2 \right) - R_s h(z) X_2 X_3 \right] + R_2 g(z) X_1 \left(X_3 + \frac{N_1 N_5}{\phi} \nabla^2 \right) \frac{\partial^2}{\partial x^2} \nabla^2 \Psi_0 \right\}, \tag{25}$$

where,

$$L_1 = \left\{ X_2 \left[X_1 \left(X_3 X_4 X_5 \nabla^2 + \frac{N_1^2}{\phi} X_5 \nabla^4 - Q \frac{P_r}{P_m} X_3 \frac{\partial^2}{\partial z^2} \nabla^2 \right) + R_s h(z) X_3 X_5 \frac{\partial^2}{\partial x^2} \right] \nabla^2 - R_0 \left[g(z) X_1 X_5 \left(X_3 + \frac{N_1 N_5}{\phi} \nabla^2 \right) \frac{\partial^2}{\partial x^2} \nabla^2 \right] \right\} \Psi_0. \tag{26}$$

The expression for R_0 , which is unmodulated Rayleigh number is obtained by taking $\Psi_0 = \sin(\pi\alpha x)\sin(\pi z)$ which satisfies the boundary conditions (20).

$$R_0 = \frac{(k^2 - R_i) \left\{ (N_3 k^2 + 2N_1) \left[(\tau k^2 - R_i) \cdot (A_1 k^2 + Q\pi^2 + R_s H(z)\alpha^2 \pi^2) \right] + \frac{N_1^2}{\phi} k^4 (\tau k^2 - R_i) \right\}}{(\tau k^2 - R_i) \alpha^2 \pi^2 G(z) \left[(N_3 k^2 + 2N_1) - \frac{N_1 N_5}{\phi} k^2 \right]} \tag{27}$$

where,

$$A_1 = \left[\Lambda \left(1 + \frac{N_1}{\Lambda \phi} \right) k^2 + Da^{-1} \right], H(z) = \int_0^1 h(z) \sin^2(\pi z) dz, G(z) = \int_0^1 g(z) \sin^2(\pi z) dz \text{ and } k^2 = \pi^2(\alpha^2 + 1).$$

Following the analysis of Siddheshwar and Pranesh [37], we get the expression for correction Rayleigh number R_{2c} as:

$$R_{2c} = \frac{-\pi^2 k^2 \alpha^2 H A_2^2 Y_1}{2 \left[\tau k^2 - R_i \right] \frac{P_r}{P_m} k^2 (Y_1^2 + Y_2^2)} \left\{ \left[N_3 k^2 + 2N_1 \right] - \frac{N_1 N_5}{\phi} k^2 \right\} \tag{28}$$

where,

$$Y_1 = k^4 \left\{ (N_3 k^2 + 2N_1) \left[A_2 \left((k^2 - R_i) B_1 - \gamma^2 B_2 \right) \right] - \gamma^2 \frac{N_2}{P_r} \left[A_2 (k^2 - R_i) B_2 - B_1 \right] \right\} + R_s H_1(z) \pi^2 k^2 \alpha^2 \left[(N_3 k^2 + 2N_1) B_3 - \gamma^2 \frac{N_2}{P_r} B_4 \right] - \frac{N_1^2}{\phi} k^6 \left[(k^2 - R_i) B_1 - \gamma^2 B_2 \right] - R_0 G_1(z) \left\{ \pi^2 k^2 \alpha^2 \left[(N_3 k^2 + 2N_1) B_5 - \gamma^2 \frac{N_2}{P_r} B_6 \right] + \frac{N_1 N_5}{\phi} \pi^2 k^6 \alpha^2 B_1 \right\} + Q \frac{P_r}{P_m} \pi^2 \left[(N_3 k^2 + 2N_1) B_5 - \gamma^2 \frac{N_2}{P_r} B_6 \right],$$

$$Y_2 = -\gamma \left[k^4 \left\{ (N_3 k^2 + 2N_1) \left[(k^2 - R_i) B_2 + B_1 \right] + \frac{1}{\phi P_r} \left[(k^2 - R_i) B_1 - \gamma^2 B_2 \right] + \frac{N_2}{P_r} \left[A_2 (k^2 - R_i) B_1 - \gamma^2 B_2 \right] - \frac{\gamma^2}{\phi P_r} \left[(k^2 - R_i) B_2 + B_1 \right] \right\} + R_s H_1(z) \pi^2 k^2 \alpha^2 \left[(N_3 k^2 + 2N_1) B_4 + \frac{N_2}{P_r} B_3 \right] - \frac{N_1^2}{\phi} k^6 \left[(k^2 - R_i) B_2 + B_1 \right] + Q \frac{P_r}{P_m} \pi^2 \left[(N_3 k^2 + 2N_1) B_6 + \frac{N_2}{P_r} B_5 \right] - R_0 G_1(z) \left\{ \pi^2 k^2 \alpha^2 \left[(N_3 k^2 + 2N_1) B_2 + \frac{N_2}{P_r} B_1 \right] + \frac{N_1 N_5}{\phi} k^2 B_2 \right\} \right],$$

$$A_2 = \frac{P_r}{P_m} k^2 \left(\frac{k^2 - \tau R_i}{\tau} \right) \left(R_0 G(z) \left[N_3 k^2 + 2N_1 \right] - \frac{N_1 N_5}{\phi} k^2 \right) + \frac{N_1 N_5}{\phi} k^2 \gamma^2 - R_s H(z) \left[k^2 - R_i \right] \left[N_3 k^2 + 2N_1 \right] \frac{P_r}{P_m} k^2,$$

$$B_1 = \frac{P_r}{P_m} k^2 (\tau k^2 - R_i) - \gamma^2, B_2 = (\tau k^2 - R_i) + \frac{P_r}{P_m} k^2, B_3 = \frac{P_r}{P_m} k^2 (k^2 - R_i) - \gamma^2, B_4 = (k^2 - R_i) + \frac{P_r}{P_m} k^2, B_5 = (\tau k^2 - R_i) (k^2 - R_i) - \gamma^2, B_6 = (\tau k^2 - R_i) + (k^2 - R_i) \text{ and } H = \frac{4\pi^2 - R_i}{2\pi^2}.$$

C. Non-Linear Analyses

The phenomenon of non-linear analysis is required to measure or interpret the results such as: rate of heat transport, rate of mass transport, convection amplitudes and so on. The heat and mass transport of the system is determined as a function of Rayleigh number, commonly called as Nusselt and Sherwood number denoted by Nu and Sh respectively. A strong convection can be measured using heat and mass flux, where the physical mechanism of fluid can be understood in a better way with less amount of mathematical analysis.

The finite amplitude free convection is carried out by the truncated Fourier series representation by taking

$$\Psi(x, y, t) = A(t) \sin(\pi\alpha x) \sin(\pi z), \tag{29}$$

$$\omega_y(x, y, t) = B(t) \sin(\pi\alpha x) \sin(\pi z), \tag{30}$$

$$T(x, y, t) = E(t) \cos(\pi\alpha x) \sin(\pi z) + F(t) \sin(2\pi z), \tag{31}$$

$$C(x, y, t) = J(t) \cos(\pi\alpha x) \sin(\pi z) + M(t) \sin(2\pi z), \tag{32}$$

$$\Phi(x, z, t) = P(t) \sin(\pi\alpha x) \cos(\pi z) + S(t) \sin(2\pi\alpha x). \tag{33}$$

where A, B, E, F, J, M, P and S describes the amplitudes which are time dependent and are obtained from the system dynamics.

Substituting equations (29)-(33) into equations (14)-(18) and equating the co-efficients of like terms we get the following eighth order differential equations that describe the non-linear non-autonomous Lorenz system:

$$\dot{A}(t) = \frac{-R[1 + \epsilon \cos(\gamma t)] \pi \alpha \phi P_r}{k^2} E(t) - Da^{-1} (\phi P_r) A(t) + \frac{R_s [1 + \epsilon \cos(\gamma t)] \pi \alpha \phi P_r}{k^2} J(t) - \Lambda \left(1 + \frac{N_1}{\Lambda \phi} \right) \pi P_r k^2 A(t) - N_1 \phi P_r B(t) - \frac{Q P_r^2 \phi}{P_m} P(t) - \frac{Q P_r^2 \phi \pi^2 \alpha (k^2 - 4\pi^2)}{P_m k^2} P(t) S(t), \tag{34}$$

$$\dot{B}(t) = -\frac{N_3 P_r k^2}{N_2} B(t) - \frac{N_1 P_r k^2}{N_2 \phi} A(t) - \frac{2N_1 P_r}{N_2} B(t), \tag{35}$$

$$\dot{E}(t) = -A(t)F(t)\pi^2\alpha - G(z) \left[A(t)\pi\alpha + N_5B(t)\pi\alpha \right] - N_5B(t)F(t)\pi^2\alpha - E(t)k^2 + R_iE(t), \tag{36}$$

$$\dot{F}(t) = \frac{\pi^2\alpha}{2}A(t)E(t) + \frac{N_5\pi^2\alpha}{2}B(t)E(t) - 4\pi^2F(t) + R_iF(t), \tag{37}$$

$$\dot{J}(t) = -\pi^2\alpha A(t)M(t) - H(z)\pi\alpha A(t) - \tau k^2J(t) + R_iJ(t), \tag{38}$$

$$\dot{M}(t) = \frac{\pi^2\alpha}{2}A(t)J(t) - 4\tau\pi^2M(t) + R_iM(t), \tag{39}$$

$$\dot{P}(t) = \frac{-P_r k^2}{P_m}P(t) + \pi A(t) + \pi^2\alpha A(t)S(t), \tag{40}$$

$$\dot{S}(t) = \frac{-\pi^2\alpha}{2}A(t)P(t) - \frac{P_r}{P_m}4\pi^2\alpha^2S(t), \tag{41}$$

where, the over dot denotes the time derivative.

The complete problem contains many properties given by generalized Lorenz model (36)-(43), which is uniformly bounded in time. Here we observe that the equation possess an important symmetry which are invariant under the transformation:

$$(A, B, E, F, J, M, P, S) \rightarrow (-A, -B, -E, -F, -J, -M, -P, -S), \tag{42}$$

The equations (34)-(41) must be dissipative in comparison with the original equations (1)-(8), thus having a contraction in the phase space volume, at a uniform rate given by equation below:

$$\begin{aligned} & \frac{\partial \dot{A}(t)}{\partial A(t)} + \frac{\partial \dot{B}(t)}{\partial B(t)} + \frac{\partial \dot{E}(t)}{\partial E(t)} + \frac{\partial \dot{F}(t)}{\partial F(t)} + \frac{\partial \dot{J}(t)}{\partial J(t)} + \frac{\partial \dot{M}(t)}{\partial M(t)} + \\ & \frac{\partial \dot{P}(t)}{\partial P(t)} + \frac{\partial \dot{S}(t)}{\partial S(t)} = - \left[\Lambda \left(1 + \frac{N_1}{\Lambda\phi} \right) \phi P_r k^2 + \frac{N_3 P_r k^2}{N_2} + \right. \\ & \left. \frac{2N_1 P_r}{N_2} + k^2 + (4\pi^2 - R_i) + (\tau k^2 - R_i) + (4\tau\pi^2 - R_i) + \right. \\ & \left. \frac{P_r}{P_m} k^2 + \frac{P_r}{P_m} 4\pi^2 \alpha^2 \right]. \end{aligned} \tag{43}$$

1) *Heat and Mass transport:* Transport of heat and mass is an important study in fluid convection, because the increase in Rayleigh number at the onset of convection is easily found by both heat and mass transport in the system. The Nusselt and Sherwood numbers gives the total heat and mass transport respectively in the system given by:

$$Nu = \frac{\left[\frac{k}{2\pi} \int_0^{\frac{2\pi}{k}} (1-z+T)_z dx \right]_{z=0}}{\left[\frac{k}{2\pi} \int_0^{\frac{2\pi}{k}} (1-z)_z dx \right]_{z=0}}. \tag{44}$$

Substituting equation (44) into (43) and solving it we get Nu which represents Nusselt number:

$$Nu = [1 - 2\pi F(t)]. \tag{45}$$

$$Sh = \frac{\left[\frac{k}{2\pi} \int_0^{\frac{2\pi}{k}} (1-z+C)_z dx \right]_{z=0}}{\left[\frac{k}{2\pi} \int_0^{\frac{2\pi}{k}} (1-z)_z dx \right]_{z=0}}. \tag{46}$$

Substituting equation (46) into (43) and solving it we get Sh which represents Sherwood number:

$$Sh = [1 - 2\pi M(t)]. \tag{47}$$

TABLE II: Values of R_c, \bar{Nu} and \bar{Sh} for different values of N_1, R_i and Q in case of modulation and without modulation

			Without Modulation $\epsilon = 0$			With Modulation $\epsilon = 0.1$		
N_1	R_i	Q	R_c	\bar{Nu}	\bar{Sh}	R_c	\bar{Nu}	\bar{Sh}
0	-2	0	3359.23	1.83638	1.69595	3359.30	1.8385	1.69549
0.1			3525.61	1.83755	1.69439	3525.68	1.8393	1.69439
0.5			4264.99	1.84127	1.68694	4264.10	1.84244	1.68769
0	-2	10	3934.6	1.8462	1.70388	3934.77	1.84723	1.70385
0.1			4117.69	1.84749	1.70266	4117.81	1.84812	1.70286
0.5			4931.34	1.85119	1.69687	4931.52	1.85103	1.69733
0	-1	0	3095.75	1.85793	1.83237	3095.80	1.85605	1.83293
0.1			3248.82	1.85884	1.83157	3248.88	1.85709	1.83226
0.5			3928.83	1.86194	1.82273	3928.92	1.86073	1.82431
0	-1	10	3637.11	1.86817	1.84087	3637.20	1.86324	1.84274
0.1			3805.84	1.86918	1.84047	3805.94	1.86463	1.84194
0.5			4555.44	1.87242	1.83413	4555.59	1.86908	1.83659
0	0	0	2839.24	1.88052	2.04092	2839.28	1.87965	2.04069
0.1			2979.37	1.88124	2.03769	2979.42	1.88042	2.03793
0.5			3601.64	1.88379	2.02718	3601.71	1.88323	2.02784
0	0	10	3347.14	1.89077	2.04968	3347.22	1.88744	2.05044
0.1			3501.9	1.89161	2.04751	3501.98	1.88849	2.04974
0.5			4189.16	1.89447	2.0409	4189.28	1.89206	2.04236
0	1	0	2589.5	1.90431	2.38328	2589.53	1.90421	2.38183
0.1			2717.03	1.90488	2.38438	2717.03	1.90478	2.38294
0.5			3283.16	1.90698	2.37749	3283.22	1.90695	2.37769
0	1	10	3064.45	1.91447	2.39484	3064.51	1.91264	2.39645
0.1			3205.6	1.91517	2.39442	3205.67	1.91345	2.39363
0.5			3832.2	1.91765	2.39221	3832.29	1.91634	2.39409
0	2	0	2346.23	1.92928	3.09949	2346.25	1.93132	3.09844
0.1			2461.51	1.92979	3.10407	2461.54	1.93175	3.09788
0.5			2973.03	1.93156	3.07167	2973.07	1.93326	3.06403
0	2	10	2788.69	1.93963	3.10424	2788.74	1.94201	3.10377
0.1			2916.6	1.94023	3.11812	2916.65	1.94252	3.11315
0.5			3484.13	1.9423	3.08776	3484.20	1.94432	3.08195

III. RESULTS AND DISCUSSION

In a thermal convection, the presence of internal heat and concentration source has an important application in the field of engineering. In this paper the effect of temperature and concentration dependent internal energy source, along with gravity modulation and magnetic field in a micropolar fluid over a porous medium is investigated using both linear and non-linear analysis. The expression for the critical Rayleigh and correction Rayleigh number as a function of $N_1, N_2, N_3, N_5, R_i, R_s, \tau, Q, P_r, P_m, Da, \Lambda$, and ϕ are obtained using regular perturbation method for linear analysis case.

The results obtained in linear analysis are depicted in figures 2 to 14. Before discussing the results obtained, we make some comments on parameters $N_1, N_2, N_3, N_5, R_i, R_s, \tau, Q, P_r, P_m, Da, \Lambda$ and ϕ . The parameters N_1, N_2, N_3 and N_5 arises due to suspended particles. Because of Clausius-Duhem inequality (see Siddheshwar and Pranesh [37]) these parameters are non-negative, have couple stress which is more significant for small values of N_3 , it indicates that $0 < N_1 \leq 1$, N_3 is a small positive real number and N_2 and N_5 are positive real number. Low amplitude gravity modulation is considered for the study. From figures we found that R_{2c} remains positive for all

frequency of gravity modulation. For small values of γ , R_{2c} increases with increase in γ , for moderate values of γ , R_{2c} decreases with increase in γ and for large values of γ , R_{2c} becomes 0. Thus small values of the frequency stabilizes the system, moderate values of frequency destabilizes the system and for larger values of frequency the effect of modulation disappears. Let $\gamma_m = \gamma_0$ be the frequency at which R_{2c} changes from stabilizing to destabilizing. The parameters Λ , D_a , ϕ arises due to porous and the parameters Q and P_m arises due to presence of magnetic field. The range of values of these parameters to analyse the problem is taken as a standard value. The parameter R_i arises due to heat and concentration source. It should be noted that the strength of both the source is taken to be same and moderate values are considered. $R_i > 0$ and $R_i < 0$ respectively represent the source and sink. The moderate values of R_s are considered and the value of τ is taken as < 1 , because heat diffusivity is more compare to solute diffusivity. Because of the presence of suspended particles due to which viscosity increases, the P_r value is taken greater than that of the fluid without suspensions.

Figures (2)–(5) are the plots of R_{2c} versus N_1, N_2, N_3 and N_5 respectively. From figure (2) we observe that increases in N_1 , increase the concentration of the suspended particles, these particle consumes more energy, thus delaying the onset of convection. Therefore N_1 stabilizes the system. From figure (3) we see that increases in N_2 , increases the inertia of the fluid. N_2 increases for small values of γ , making the system stable. Whereas N_2 makes the system unstable for moderate values of γ . It should be noted here N_2 affects only R_{2c} , but not R_0 (see eqn[29]). From figure (4), we find that when N_3 increases, R_{2c} decreases, this is because when N_3 increases the coupling between vorticity and spin increases and hence makes the system unstable. In figure (5), we notice that increase in N_5 , heat supplied to the fluid increases and because of presence of microelements, heat transport is decreased thus delaying the onset of convection. Thus increase in N_5 stabilizes the system.

Figure (6) depicts the effects of internal source/sink parameter R_i on R_{2c} . In this paper the values of R_i are taken in such a way that the buoyancy force will not dominate heat source or sink. We observe that the impact of increases in R_i positively is to suppress the R_{2c} . Thus the internal source energy destabilizes the system, whereas increase in heat sink ($R_i < 0$) stabilizes the system.

Figure (7) and (8) shows the effects of solute Rayleigh number R_s and diffusivity ratio τ on R_{2c} . Increase in R_s increases R_{2c} indicating that the effect of R_s is to inhibit the onset of double diffusive convection. Positive value of R_s are considered indicating the concentration are added from below. Increase in τ , advances the convection, indicating the effect of τ is to destabilize the system. Values of τ are taken < 1 as discussed earlier.

Figures (9), (10) and (11) respectively shows the effects of Chandrasekhar number Q , prandtl number P_r and magnetic prandtl number P_m on R_{2c} . We observe that increase in Q delays the onset of convection thus stabilizing the system. This is because increase in Q increases the Lorentz force in horizontal direction, which will not allow the fluid more freely in the vertical direction, hence Q stabilizes the system. For small values of γ , P_r destabilizes and for moderate

values P_r stabilizes the system and P_m in general stabilizes the system (see Siddheshwar and Pranesh [36]).

Figures (12), (13) and (14) respectively shows the effects of modified viscosity ratio Λ , Darcy number D_a and porosity parameter ϕ . We observe that the effect of Λ is to stabilize the system whereas increase in D_a and ϕ destabilizes the system.

The heat and mass transport across the porous medium plays an important role in double diffusive convection. This is also one of the objective of the paper. Heat and mass transport across the fluid layer are quantified by Nusselt number (Nu) and Sherwood number (Sh) respectively. The effect of different parameters on Nu and Sh with respect to time 't' is considered by solving the non-autonomous differential equations with appropriate initial condition and results obtained are depicted in figures (15)–(27). From the figures it is observed that Nusselt number and Sherwood number starts with $Nu=Sh=1$, which signifies the conduction state. As time progress Nu and Sh increases which show the convective regime has taken place. It is also observed that Nu and Sh remains oscillating for small time. However for large time Nu levels off to a steady-state value, whereas Sh remains oscillating because of sudden chaos that has taken place. Also from the figures we found that mass transport is more compare to heat transport.

From figures (15)–(27) following observations are made: Increase in N_1, N_2 and N_5 decreases Nu , indicating these parameters stabilizes the system (as noted earlier) and hence reduces the heat transport. However, increase in these parameters increases the mass transport (i.e. increases Sh) due to presence of suspended particles. Increase in N_3 destabilizes the system thereby increases the heat transport and decreases the mass transport. An increase in R_i increases Nu indicating the heat transport is more for higher values of R_i and reconfirming it destabilizes the thermal instability. It is important to note that heat and concentration source, increases the heat transport whereas heat and concentration sink, decreases the mass transport. It is interesting to note that, the increase in R_s decreases both Nu and Sh indicating the reduced heat and mass transport, this is due to the fact that inhibiting effect of solute gradient is reduced because of increase in thermal Rayleigh number. Increase in τ we observe that increases heat and mass transport. Increase in Q decreases Nu and Sh which indicates, the strong magnetic field leads to decrease in heat and mass transport. Increase in P_r and P_m reduces the heat transport and increases the mass transport. The porous parameters D_a and ϕ decreases the heat transport and increases the mass transport, whereas Λ has reverse effect of that of D_a and ϕ .

Table II, documents the effects of N_1, R_i and Q on critical Rayleigh number R_c , average Nusselt number \overline{Nu} and average Sherwood number \overline{Sh} . The following are the results observed from the table:

- | | |
|---|--|
| 1. $R_c _{N_1 \neq 0} > R_c _{N_1=0}$, | 8. $\overline{Nu} _{Q \neq 0} > \overline{Nu} _{Q=0}$, |
| 2. $R_c _{R_i > 0} < R_c _{R_i=0}$, | 9. $\overline{Sh} _{N_1 \neq 0} < \overline{Sh} _{N_1=0}$, |
| 3. $R_c _{R_i < 0} > R_c _{R_i=0}$, | 10. $\overline{Sh} _{R_i > 0} > \overline{Sh} _{R_i=0}$, |
| 4. $R_c _{Q \neq 0} > R_c _{Q=0}$, | 11. $\overline{Sh} _{R_i < 0} < \overline{Sh} _{R_i=0}$, |
| 5. $\overline{Nu} _{N_1 \neq 0} > \overline{Nu} _{N_1=0}$, | 12. $\overline{Sh} _{Q \neq 0} > \overline{Sh} _{Q=0}$, |
| 6. $\overline{Nu} _{R_i > 0} > \overline{Nu} _{R_i=0}$, | 13. $\overline{Nu} _{\epsilon=0} > \overline{Nu} _{\epsilon \neq 0}$, |
| 7. $\overline{Nu} _{R_i < 0} < \overline{Nu} _{R_i=0}$, | 14. $\overline{Sh} _{\epsilon=0} < \overline{Sh} _{\epsilon \neq 0}$. |

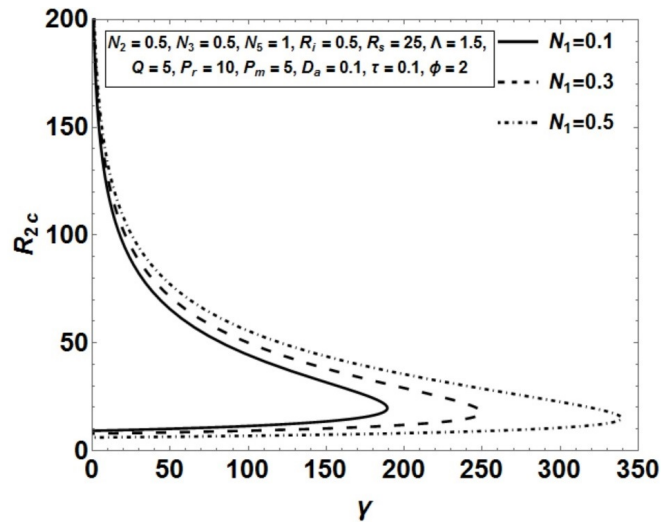


Fig. 2: Plot of Frequency of Modulation γ versus Critical Rayleigh Number R_{2c} for different values of Coupling Parameter N_1 .

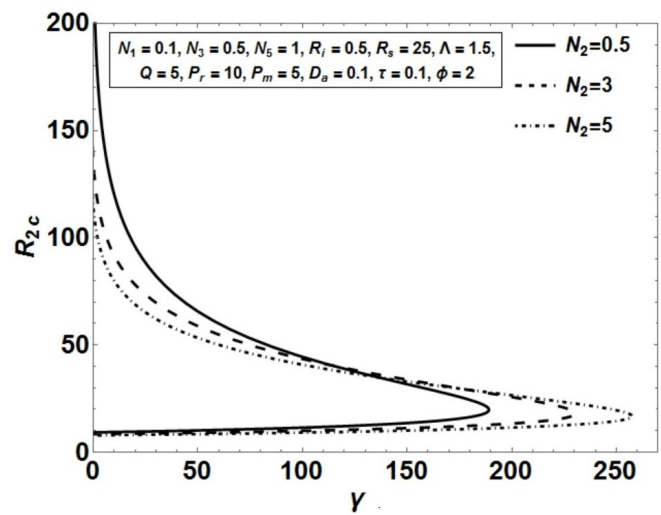


Fig. 3: Plot of Frequency of Modulation γ versus Critical Rayleigh Number R_{2c} for different values of Inertia Parameter N_2 .

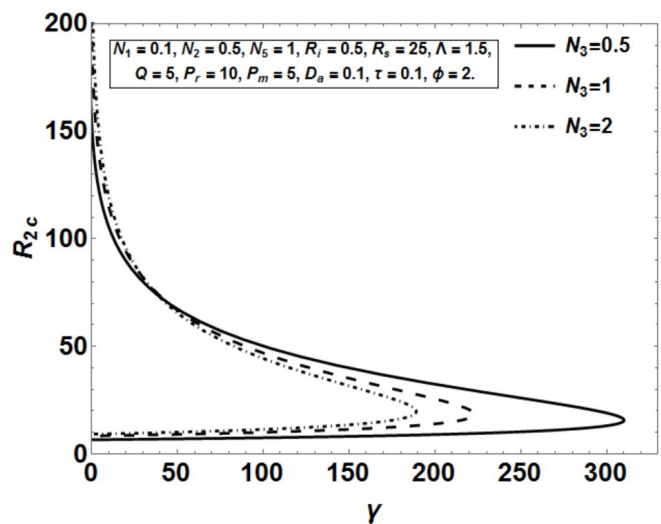


Fig. 4: Plot of Frequency of Modulation γ versus Critical Rayleigh Number R_{2c} for different values of Couple Stress Parameter N_3 .

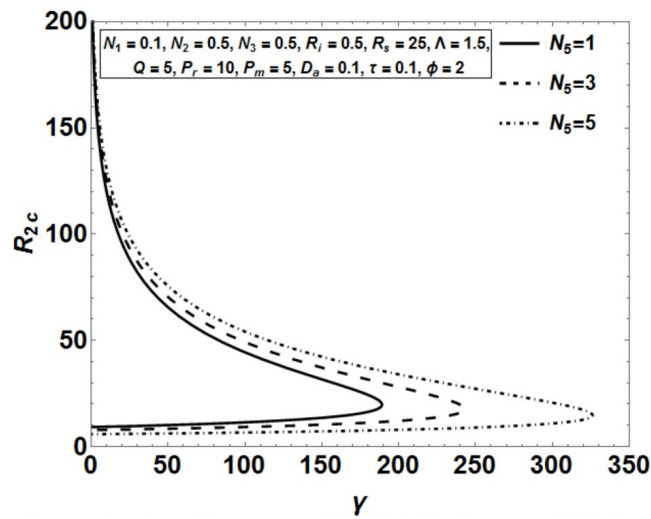


Fig. 5: Plot of Frequency of Modulation γ versus Critical Rayleigh Number R_{2c} for different values of Micropolar Heat Conduction Parameter N_5 .

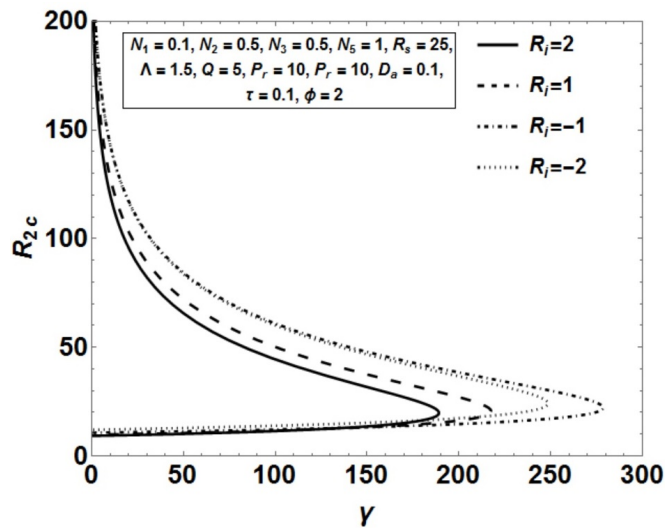


Fig. 6: Plot of Frequency of Modulation γ versus Critical Rayleigh Number R_{2c} for different values of Internal Rayleigh Number R_i .

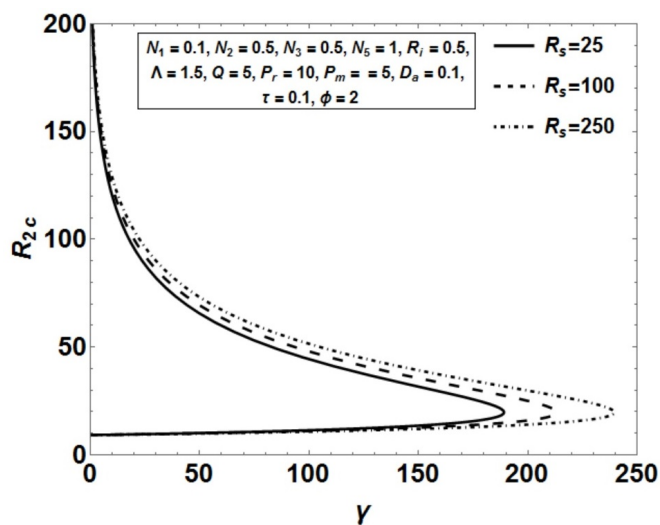


Fig. 7: Plot of Frequency of Modulation γ versus Critical Rayleigh Number R_{2c} for different values of Solutal Rayleigh Number R_s .

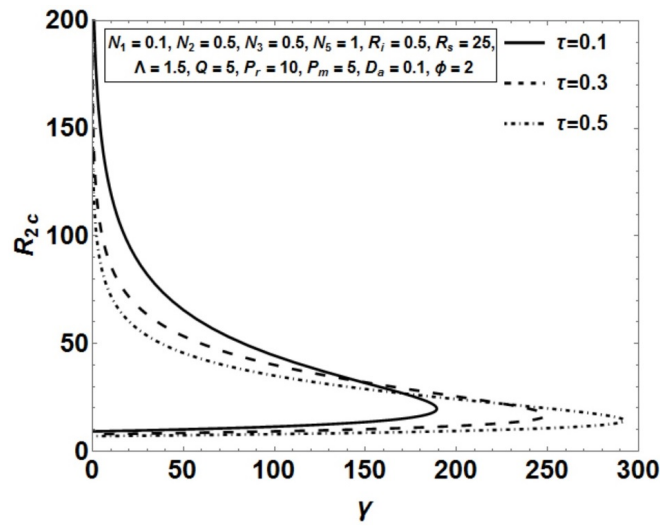


Fig. 8: Plot of Frequency of Modulation γ versus Critical Rayleigh Number R_{2c} for different values of Diffusivity Ratio τ .

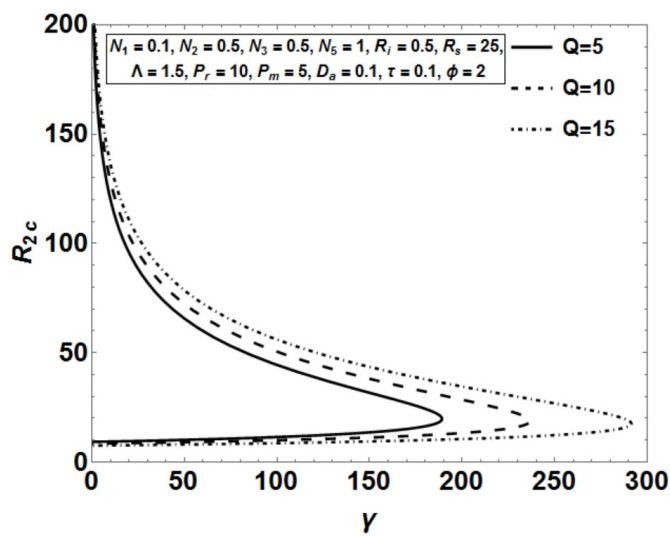


Fig. 9: Plot of Frequency of Modulation γ versus Critical Rayleigh Number R_{2c} for different values of Chandrasekhar Number Q .

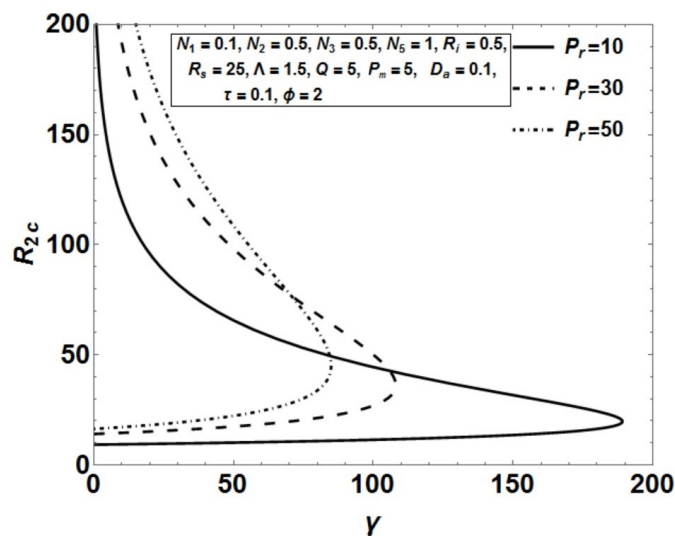


Fig. 10: Plot of Frequency of Modulation γ versus Critical Rayleigh Number R_{2c} for different values of Prandtl Number P_r .

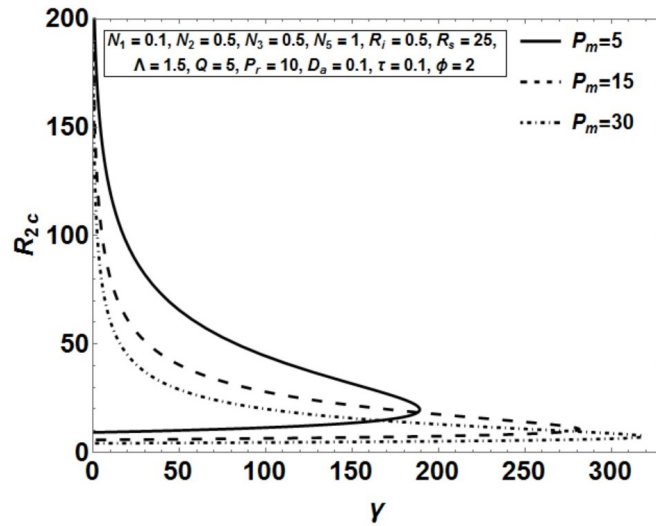


Fig. 11: Plot of Frequency of Modulation γ versus Critical Rayleigh Number R_{2c} for different values of Magnetic Prandtl Number P_m .

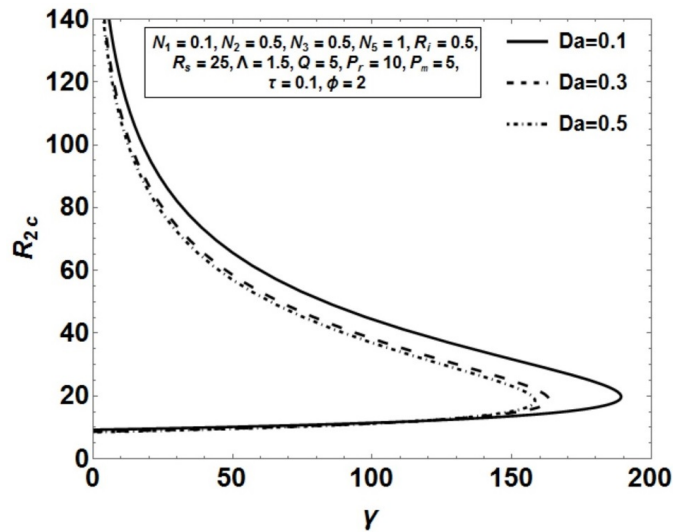


Fig. 12: Plot of Frequency of Modulation γ versus Critical Rayleigh Number R_{2c} for different values of Darcy Number Da .

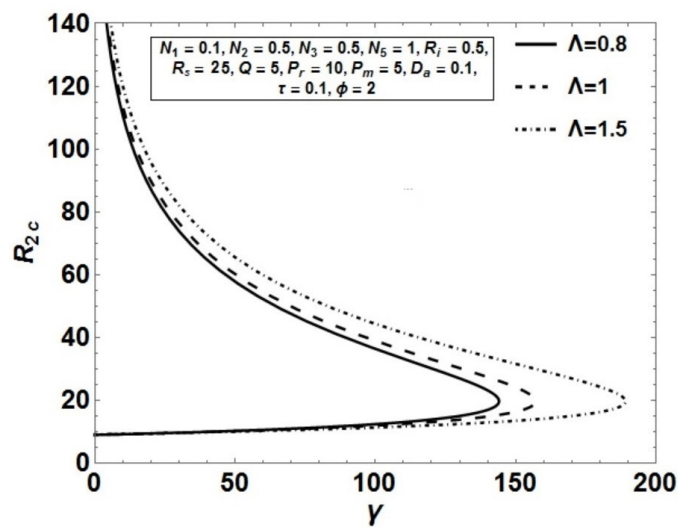


Fig. 13: Plot of Frequency of Modulation γ versus Critical Rayleigh Number R_{2c} for different values of Modified Viscosity Ratio Λ .

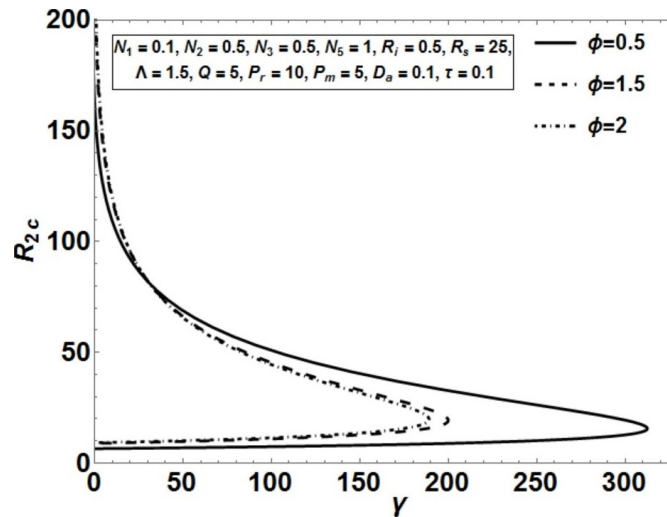


Fig. 14: Plot of Frequency of Modulation γ versus Critical Rayleigh Number R_{2c} for different values of Porosity ϕ .

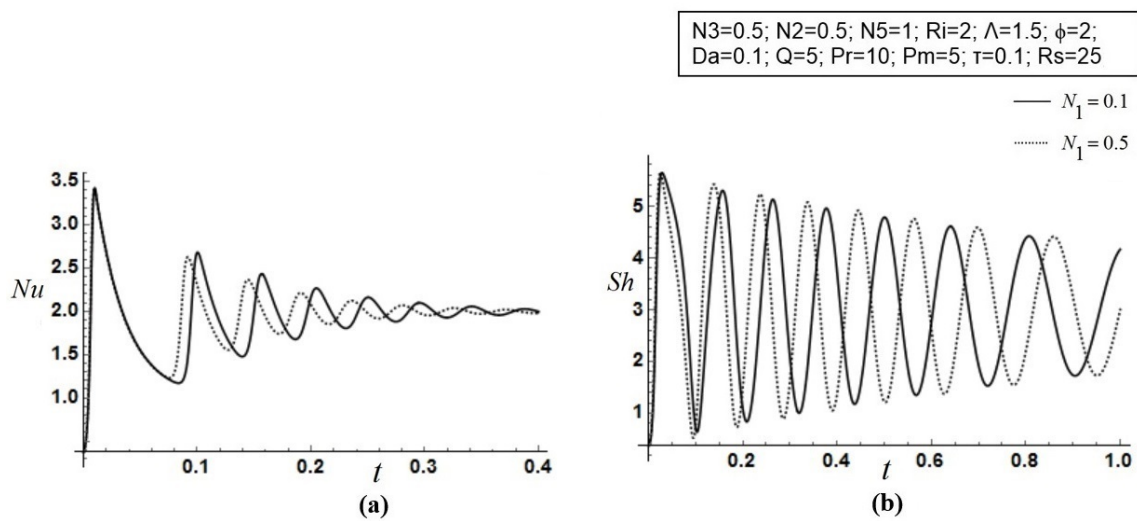


Fig. 15: Plot of Nusselt Number Nu and Sherwood Number Sh versus Time t is given by (a) and (b) respectively for different values of Coupling Parameter N_1 .

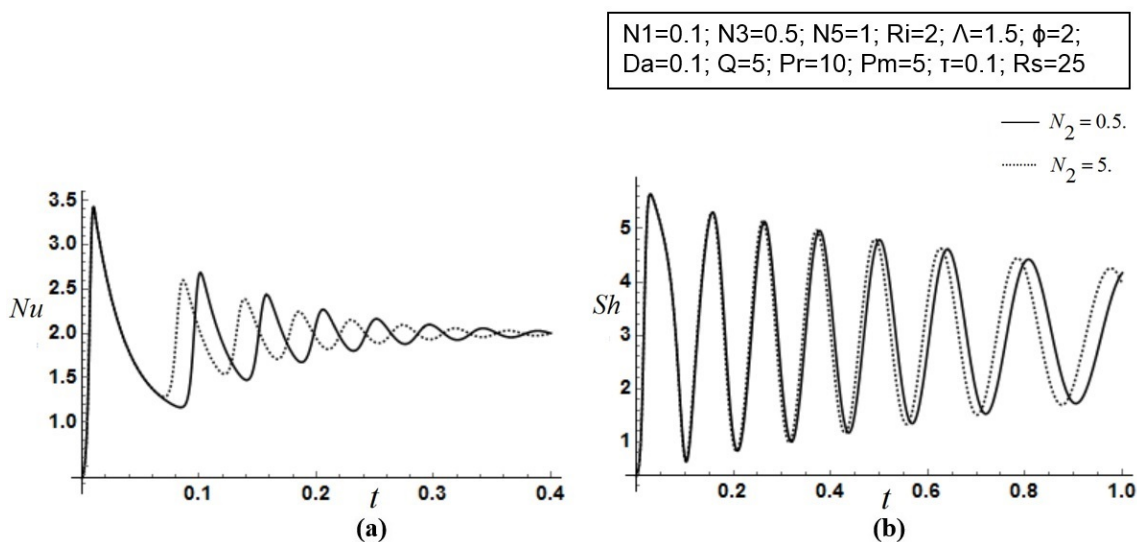


Fig. 16: Plot of Nusselt Number Nu and Sherwood Number Sh versus Time t is given by (a) and (b) respectively for different values of Inertia Parameter N_2 .

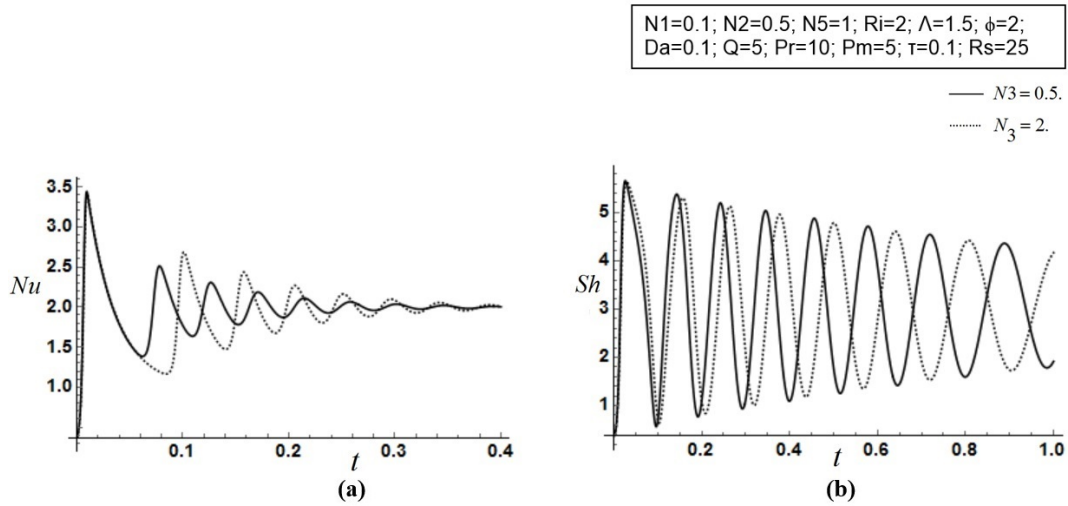


Fig. 17: Plot of Nusselt Number Nu and Sherwood Number Sh versus Time t is given by (a) and (b) respectively for different values of Couple Stress Parameter N_3 .

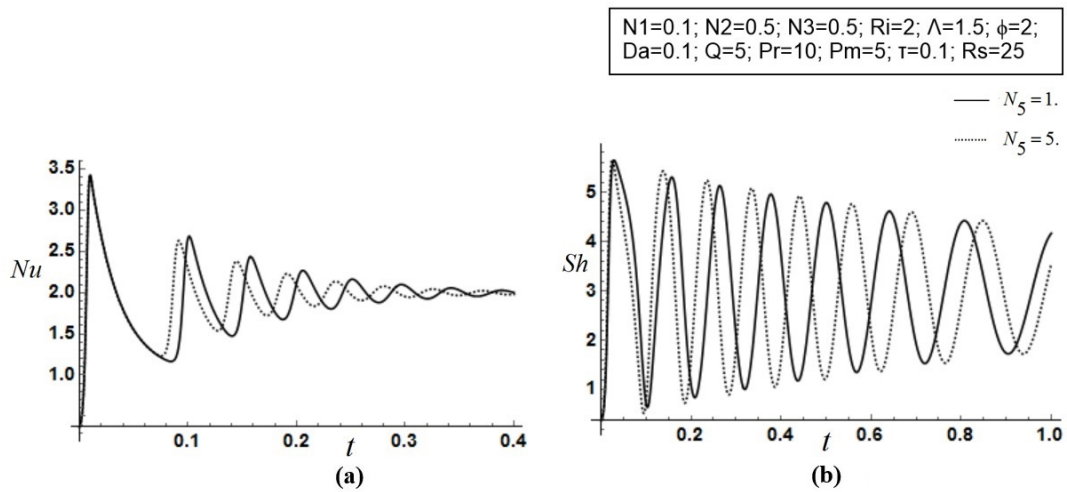


Fig. 18: Plot of Nusselt Number Nu and Sherwood Number Sh versus Time t is given by (a) and (b) respectively for different values of Micropolar Heat Conduction Parameter N_5 .

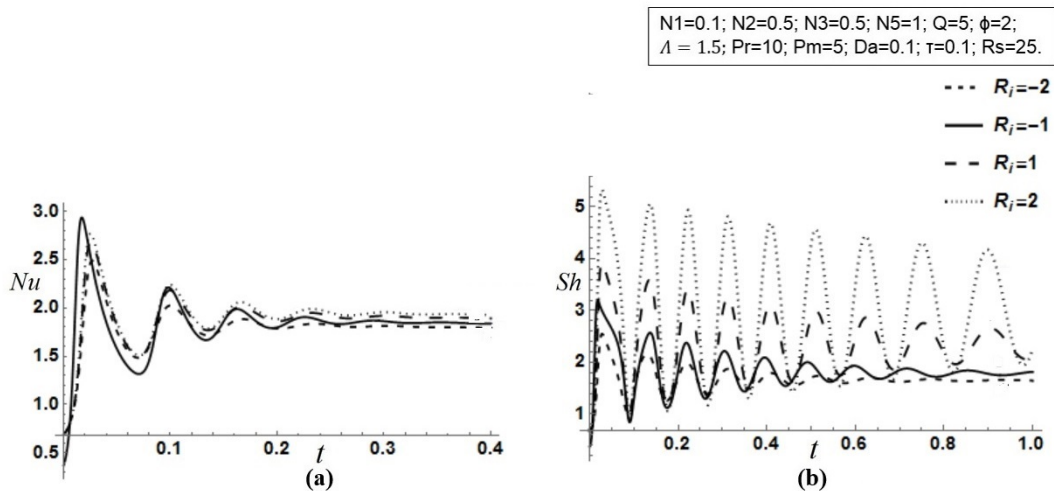


Fig. 19: Plot of Nusselt Number Nu and Sherwood Number Sh versus Time t is given by (a) and (b) respectively for different values of Internal Rayleigh Number R_i .

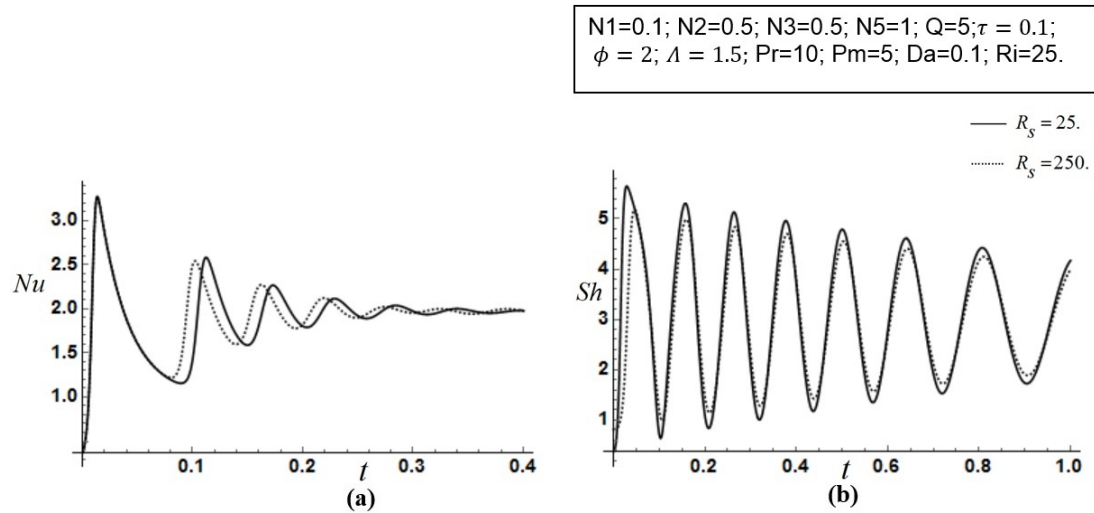


Fig. 20: Plot of Nusselt Number Nu and Sherwood Number Sh versus Time t is given by (a) and (b) respectively for different values of Solutal Rayleigh Number R_s .

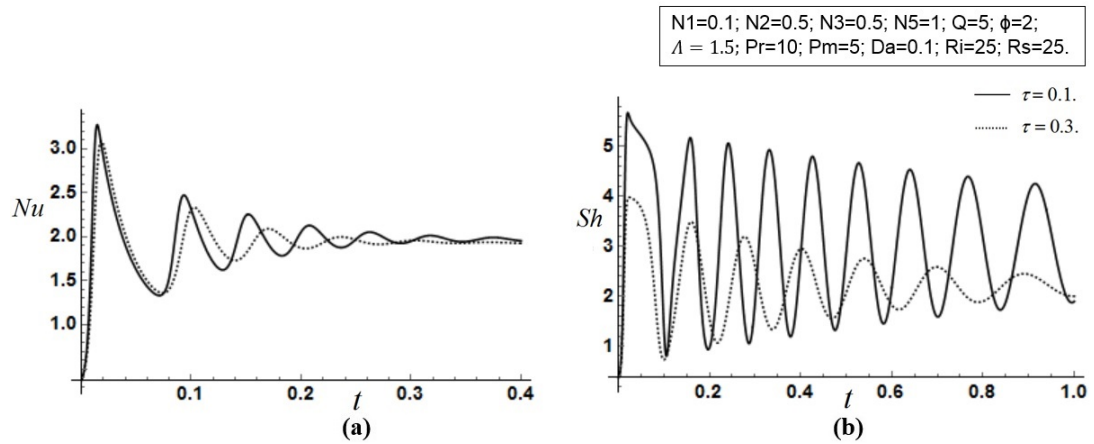


Fig. 21: Plot of Nusselt Number Nu and Sherwood Number Sh versus Time t is given by (a) and (b) respectively for different values of Diffusivity Ratio τ .

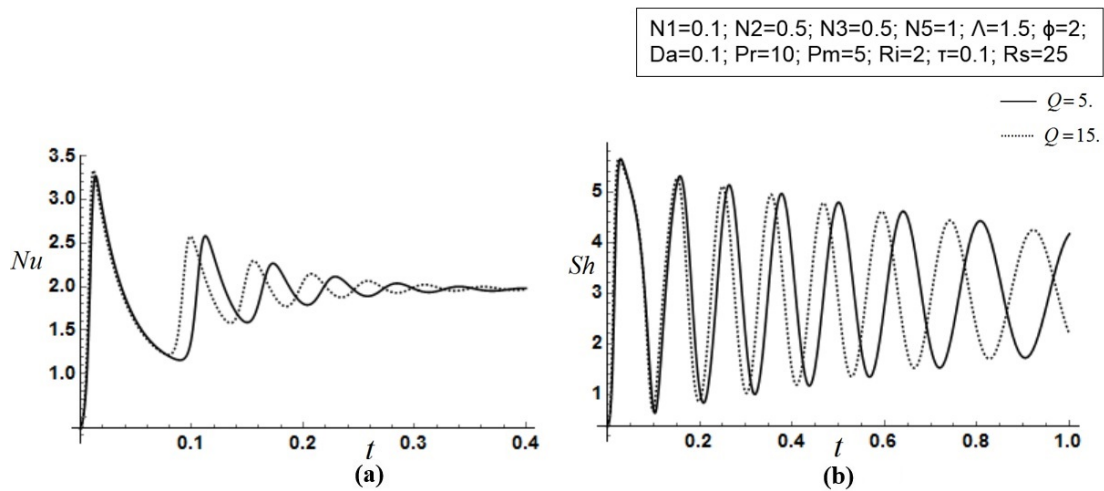


Fig. 22: Plot of Nusselt Number Nu and Sherwood Number Sh versus Time t is given by (a) and (b) respectively for different values of Chandrasekhar Number Q .

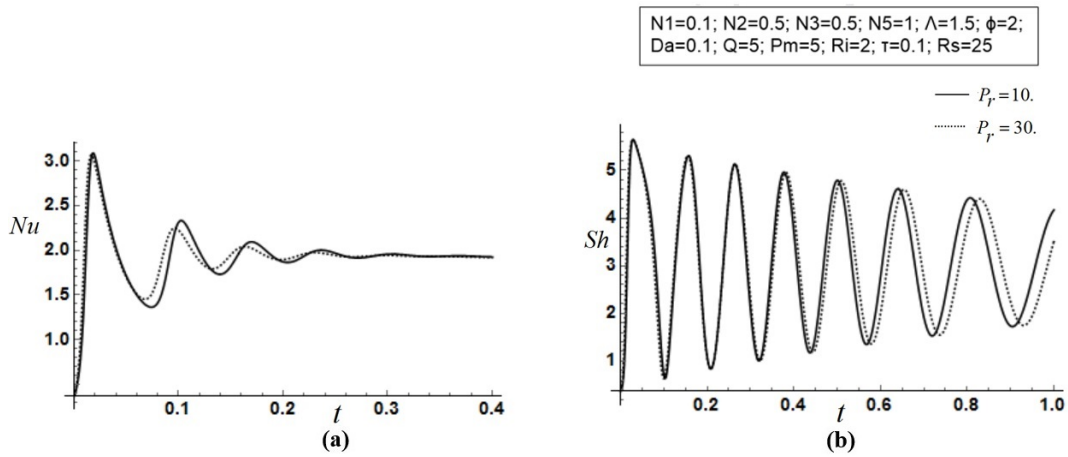


Fig. 23: Plot of Nusselt Number Nu and Sherwood Number Sh versus Time t is given by (a) and (b) respectively for different values of Prandtl Number P_r .

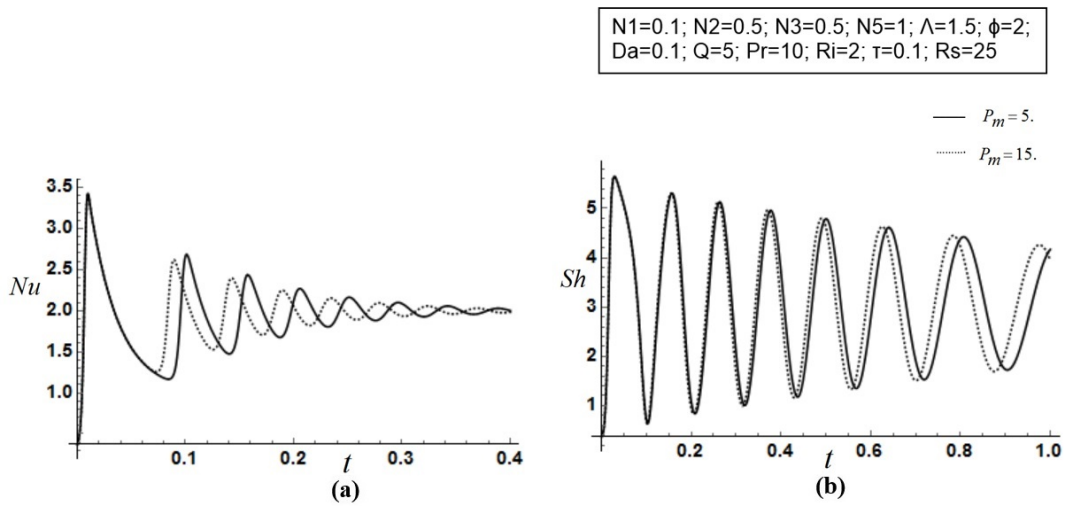


Fig. 24: Plot of Nusselt Number Nu and Sherwood Number Sh versus Time t is given by (a) and (b) respectively for different values of Magnetic Prandtl Number P_m .

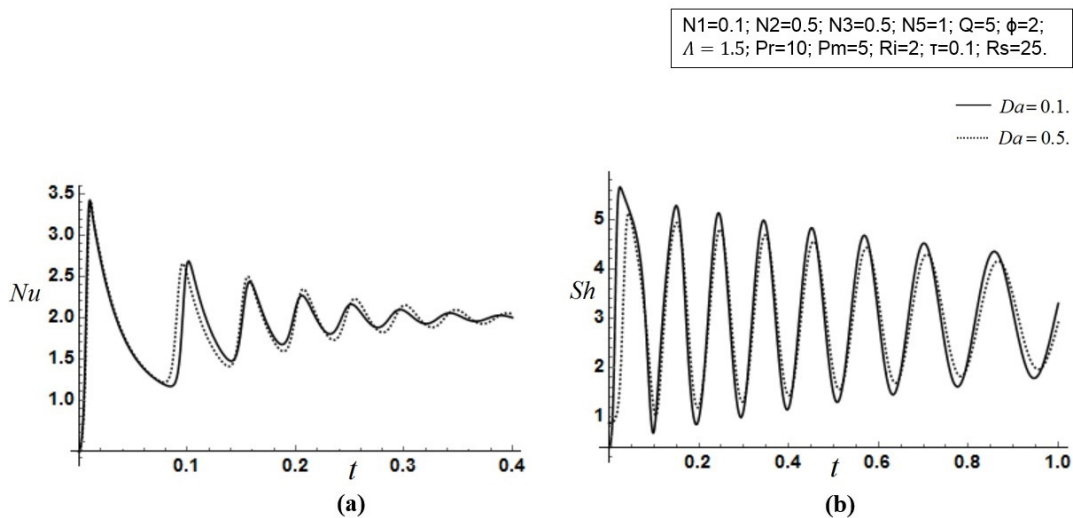


Fig. 25: Plot of Nusselt Number Nu and Sherwood Number Sh versus Time t is given by (a) and (b) respectively for different values of Darcy Number Da .

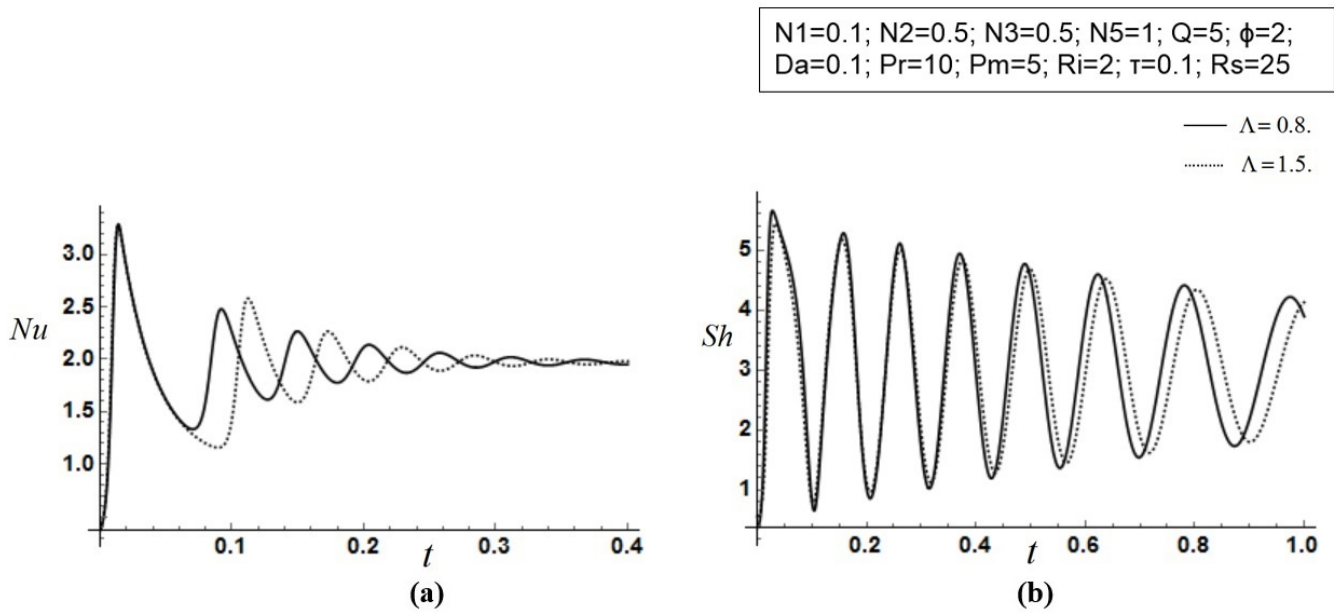


Fig. 26: Plot of Nusselt Number Nu and Sherwood Number Sh versus Time t is given by (a) and (b) respectively for different values of Modified Viscosity Ratio Λ .

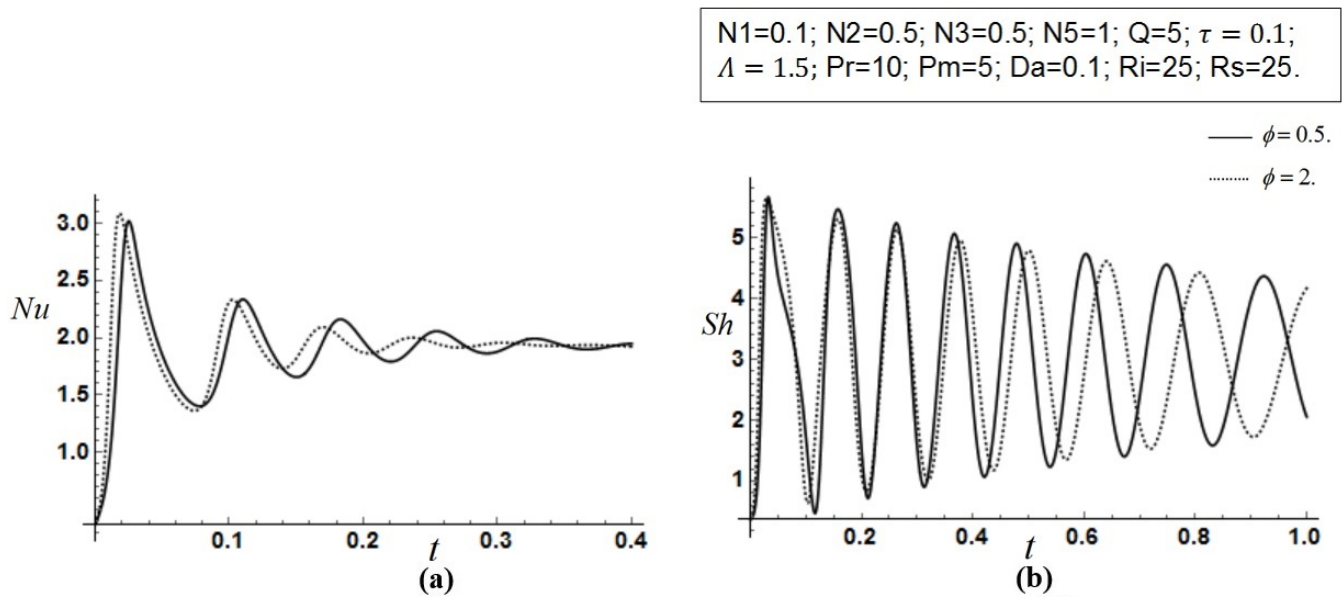


Fig. 27: Plot of Nusselt Number Nu and Sherwood Number Sh versus Time t is given by (a) and (b) respectively for different values of Porosity ϕ .

IV. CONCLUSION

The effect of heat and concentration energy source/sink on double diffusive convection in a micropolar fluid, in the presence of magnetic field and gravity modulation is studied with porous medium. The expression for Rayleigh number and correction Rayleigh number is obtained by regular perturbation method. The Nusselt and Sherwood number are obtained using the solution of Lorenz equations. The following conclusions are drawn from the study:

- The parameters $N_1, N_5, R_s, Q, P_r, P_m$ and Λ stabilizes the system hence delaying the onset of convection.
- The parameters N_2, N_3, R_i, τ, D_a and ϕ destabilizes the system by advancing the onset of convection.
- The parameters N_1, N_2, N_5, P_r, P_m and τ decreases the heat transport, whereas as an reverse effect on mass transport.
- The parameter R_i increases both heat and mass transport.
- Both heat and mass transport is decreased by the parameters R_s, Q, D_a and ϕ .
- The parameters N_3 and Λ increases the heat transport, whereas decreases the mass transport.
- Mass transport is more compare to heat transport.
- The average Nusselt number \overline{Nu} with modulation is less compared to without modulation.
- The average Sherwood number \overline{Sh} with modulation is more compared to without modulation.
- The average heat transport increases, whereas average mass transport decreases when micron sized suspended particles are added into clear fluid.

REFERENCES

- [1] D. A. Nield and A. Bejan, *Convection in porous media 8.1*. Springer, 2017.
- [2] M. A. Sheremet, I. Pop, and N. Bachok, "Effect of thermal dispersion on transient natural convection in a wavy-walled porous cavity filled with a nanofluid: Tiwari and das' nanofluid model," *International Journal of Heat and Mass Transfer*, vol. 92, pp. 1053–1060, 2016.
- [3] C. Sivaraj and M. A. Sheremet, "Mhd natural convection in an inclined square porous cavity with a heat conducting solid block," *Journal of Magnetism and Magnetic Materials*, vol. 426, pp. 351–360, 2017.
- [4] I. V. Miroshnichenko, M. A. Sheremet, H. F. Oztop, and A. N. Hamdeh, "Natural convection of alumina-water nanofluid in an open cavity having multiple porous layers," *International Journal of Heat and Mass Transfer*, vol. 125, pp. 648–657, 2018.
- [5] M. Izadi, S. Sinaei, S. A. Mehryan, H. F. Oztop, and A. N. Hamdeh, "Natural convection of a nanofluid between two eccentric cylinders saturated by porous material: Buongiorno's two phase model," *International Journal of Heat and Mass Transfer*, vol. 127, pp. 67–75, 2018.
- [6] J. S. Turner, "Multicomponent convection," *Annual Review of Fluid Mechanics*, vol. 17, pp. 11–44, 1985.
- [7] J. S. Turner and H. E. Huppert, "Double-diffusive convection," *Journal of Fluid Mechanics*, vol. 106, pp. 299–329, 1981.
- [8] R. Schmitt, "Double diffusion in oceanography," *Annual Review of Fluid Mechanics*, vol. 26, no. 1, pp. 255–285, 1994.
- [9] C. Chen and D. Johnson, "Double-diffusive convection: A report on an engineering foundation conference," *Journal of Fluid Mechanics*, vol. 138, pp. 405–416, 1984.
- [10] D. A. Nield, "Onset of thermohaline convection in a porous medium," *Water Resources Research*, vol. 4, pp. 553–560, 1968.
- [11] J. W. Taunton, E. N. Lightfoot, and T. Green, "Thermohaline instability and salt fingers in a porous medium," *Physics of Fluids*, vol. 15, pp. 748–753, 1972.
- [12] N. Rudraiah, P. K. Srimani, and R. Friedrich, "Finite amplitude convection in a two- component fluid saturated porous layer," *International Journal of Heat and Mass Transfer*, vol. 25, no. 5, pp. 715–722, 1982.
- [13] P. Dimos, "Double diffusive convection in a horizontal sparsely packed porous layer," *International Communications in Heat and Mass Transfer*, vol. 13, pp. 587–598, 1986.
- [14] N. D. Rosenberg and F. J. Spera, "Thermohaline convection in a porous medium heated from below," *International Journal of Heat and Mass Transfer*, vol. 35, no. 5, pp. 1261–1273, 1992.
- [15] A. V. Kuznetsov and D. A. Nield, "The effects of combined horizontal and vertical heterogeneity on the onset of convection in a porous medium: Double diffusive case," *Transport in Porous Media*, vol. 72, pp. 157–170, 2008.
- [16] D. A. Nield and A. V. Kuznetsov, "The cheng-minkowycz problem for the double-diffusive natural convective boundary layer flow in a porous medium saturated by a nanofluid," *International Journal of Heat and Mass Transfer*, vol. 54, pp. 374–378, 2011.
- [17] G. C. Rana and R. Chand, "Stability analysis of double-diffusive convection of rivlin-ericksen elastico-viscous nanofluid saturating a porous medium: A revised model," *Forsch Ingenieurwes*, 2015.
- [18] B. S. Bhadauria, P. G. Siddheshwar, A. K. Singh, and V. K. Gupta, "A local nonlinear stability analysis of modulated double diffusive stationary convection in a couple stress liquid," *Journal of Applied Fluid Mechanics*, vol. 9, no. 3, pp. 1255–1264, 2016.
- [19] A. Noreen, Z. Khan, S. Nadeem, and W. Khan, "Double-diffusive natural convective boundary-layer flow of a nanofluid over a stretching sheet with magnetic field," *International Journal of Numerical Methods for Heat and Fluid Flow*, vol. 26, no. 1, pp. 108–121, 2016.
- [20] A. J. Harfash, "Continuous dependence of double diffusive convection in a porous medium with temperature-dependent density," *Basrah Journal of Science*, vol. 37, no. 1, pp. 1–15, 2019.
- [21] A. J. Harfash, "Nonhomogeneous porosity and thermal diffusivity effects on a double-diffusive convection in anisotropic porous media," *International Journal of Nonlinear Sciences and Numerical Simulation*, vol. 17, no. 5, pp. 205–220, 2016.
- [22] P. Garaud, "Double-diffusive convection at low prandtl number," *Annual Review of Fluid Mechanics*, vol. 50, no. 1, pp. 275–298, 2017.
- [23] K. R. Raghunatha and I. S. Shivakumara, "Double-diffusive convection in an oldroyd-b fluid layer-stability of bifurcating equilibrium solutions," *Journal of Applied Fluid Mechanics*, vol. 12, no. 1, pp. 85–94, 2012.
- [24] P. M. Gresho and R. L. Sani, "The effects of gravity modulation on the stability of a heated fluid layer," *Journal of Fluid Mechanics*, vol. 40, no. 4, pp. 783–806, 1970.
- [25] B. T. Murray, S. R. Coriell, and G. B. McFadden, "The effect of gravity modulation on solutal convection during directional solidification," *Journal of Crystal Growth*, vol. 110, pp. 713–723, 1991.
- [26] B. V. Saunders, B. T. Murray, G. B. McFadden, S. R. Coriell, and A. A. Wheeler, "The effect of gravity modulation on thermosolutal convection in an infinite layer of fluid," *Physics of Fluids A Fluid Dynamics*, vol. 4, no. 6, pp. 1176–1189, 1992.
- [27] P. G. Siddheshwar, B. S. Bhadauria, and S. Alok, "An analytical study of nonlinear double-diffusive convection in a porous medium under temperature/gravity modulation," *Transport in Porous Media*, vol. 91, no. 2, pp. 585–604, 2012.
- [28] B. S. Bhadauria, I. Hashim, and P. G. Siddheshwar, "Effect of internal-heating on weakly non-linear stability analysis of rayleigh-bénard convection under g-jitter," *International Journal of Non-Linear Mechanics*, vol. 54, pp. 35–42, 2013.
- [29] B. S. Bhadauria, A. Singh, and M. K. Singh, "Chaotic convection of viscoelastic fluid in porous medium under g-jitter," *International Journal of Applied Mechanics and Engineering*, vol. 24, no. 1, pp. 37–51, 2019.
- [30] T. Maria and G. Sangeetha, "Effect of gravity modulation and internal heat generation on rayleigh-bénard convection in couple stress fluid with maxwell-cattaneo law," *International Journal of Applied Engineering Research*, vol. 13, pp. 2688–2693, 2018.
- [31] A. Purusothaman, R. C. S. Guru, and K. Murugesan, "Magnetic field and vibration effects on the onset of thermal convection in a grade fluid permeated anisotropic porous module," *Thermal Science and Engineering Progress*, vol. 10, pp. 138–146, 2019.
- [32] G. Lukaszewicz, *Micropolar fluid-theory and applications*, 1999.
- [33] G. Ahamadi, "Stability of a micropolar fluid layer heated from below," *International Journal of Applied Mechanics and Engineering*, vol. 14, pp. 81–89, 1976.
- [34] S. K. Jena and S. P. Bhattacharyya, "The effect of microstructure on the thermal convection in a rectangular box of fluid heated from below," *International Journal of Engineering and Sciences*, vol. 24, no. 1, pp. 69–78, 1986.
- [35] A. B. Datta and V. U. K. Sastry, "Thermal instability of a horizontal layer of micropolar fluid heated from below," *International Journal of Engineering Science*, vol. 14, pp. 631–637, 1976.

- [36] P. G. Siddheshwar and S. Pranesh, "Magnetoconvection in a micropolar fluid," *International Journal of Engineering Science*, vol. 36, pp. 1173–1181, 1998.
- [37] P. G. Siddheshwar and S. Pranesh, "Effect of temperature/gravity modulation on the onset of magneto-convection in electrically conducting fluids with internal angular momentum," *Journal of Magnetism and Magnetic Materials*, vol. 192, pp. 159–176, 1999.
- [38] P. G. Siddheshwar and S. Pranesh, "Effects of non-uniform temperature gradient and magnetic field on the onset of convection in fluids with suspended particles under microgravity conditions," *Indian Journal of Engineering and Materials Sciences*, vol. 8, pp. 77–83, 2001.
- [39] P. G. Siddheshwar and S. Pranesh, "Magnetoconvection in fluids with suspended particles under 1g and μg ," *Aerospace Science and Technology*, vol. 6, no. 2, pp. 105–114, 2002.
- [40] S. Pranesh and N. K. Arun, "Effect of non-uniform basic concentration gradient on the onset of double-diffusive convection in micropolar fluid," *Applied Mathematics*, vol. 3, pp. 417–424, 2012.
- [41] S. Pranesh and N. K. Arun, "Study of heat transfer in a time dependent vertically oscillating micropolar liquid," *Recent Trends in Fluid Mechanics*, vol. 5, pp. 63–74, 2018.
- [42] S. Pranesh and B. Riya, "Effect of non-uniform temperature gradient on the onset of rayleigh-bénard electro convection in a micropolar fluid," *Applied Mathematics*, vol. 3, pp. 442–450, 2012.
- [43] S. Pranesh and T. Sameena, "Linear and weakly non-linear stability analyses of double-diffusive electro- convection in a micropolar fluid," *IOSR Journal of Mathematics*, vol. 11, pp. 2278–5728, 2015.
- [44] A. A. Hill, "Double-diffusive convection in a porous medium with a concentration based internal heat source," *Proceedings of the Royal Society A: Mathematical, Physical and Engineering Sciences*, vol. 461, no. 2054, pp. 561–574, 2005.
- [45] A. Matta and A. H. Antony, "Double-diffusive convection in an inclined porous layer with a concentration-based internal heat source," *Continuum Mechanics of Thermodynamics*, vol. 30, pp. 165–173, 2018.
- [46] G. Venezian, "Effect of modulation on the onset of thermal convection," *Journal of Fluid Mechanics*, vol. 35, pp. 243–254, 1969.